Submitted to Metallurgical Transactions

LBL-1853
Preprint

DEFORMATION INDUCED ALPHA AND EPSILON MARTENSITES IN Fe-Ni-Cr SINGLE CRYSTALS

Glen Stone and Gareth Thomas

July 1973

Prepared for the U. S. Atomic Energy Commission
under Contract W-7405-ENG-48

For Reference

Not to be taken from this room

LAWRENCE BERKELEY LABORATORY
UNIVERSITY OF CALIFORNIA
BERKELEY

LBL-1853

DISCLAIMER

This document was prepared as an account of work sponsored by the United States Government. While this document is believed to contain correct information, neither the United States Government nor any agency thereof, nor the Regents of the University of California, nor any of their employees, makes any warranty, express or implied, or assumes any legal responsibility for the accuracy, completeness, or usefulness of any information, apparatus, product, or process disclosed, or represents that its use would not infringe privately owned rights. Reference herein to any specific commercial product, process, or service by its trade name, trademark, manufacturer, or otherwise, does not necessarily constitute or imply its endorsement, recommendation, or favoring by the United States Government or any agency thereof, or the Regents of the University of California. The views and opinions of authors expressed herein do not necessarily state or reflect those of the United States Government or any agency thereof or the Regents of the University of California.

0 0 0 0 3 9 0 0 9 1 5

DEFORMATION INDUCED ALPHA AND EPSILON MARTENSITES IN Fe-Ni-Cr SINGLE CRYSTALS

Glen Stone and Gareth Thomas

Inorganic Materials Research Division, Lawrence Berkeley Laboratory and Department of Materials Science and Engineering, College of Engineering; University of California, Berkeley, California 94720

ABSTRACT

An x-ray method is used in a new way so as to study how the orientation dependence of the applied stress in Fe-15^{w}/oNi-15^{w}/oCr single crystals controls the formation of specific Kurdjumov-Sachs (K-S) variants of α martensite above Ms_{γ}. It is found that the distribution of these K-S variants can be correlated to the slip systems operating in the crystal. Quantitative volume fraction measurements of α martensite present in crystals orientated for easy glide show that 80% of the martensite formed has the same K-S variant. The ε martensite forms as large sheets parallel to the austenite slip plane. Epsilon martensite is only observed in association with $\{111\}_{\gamma}$ planes that have slipped. The orientation relationship observed is the well known $\{0001\}_{\varepsilon} \parallel \{111\}_{\gamma}$. All the crystals tested in tension at 273° and 242°K did not contain α martensite, but did contain the ε phase. At 185°K crystals with $[100]_{\gamma}$, $[\bar{2}\bar{1}3]_{\gamma}$, $[\bar{1}\bar{1}2]_{\gamma}$ and $[1\bar{1}0]_{\gamma}$ tensile axes were pulled to 5% tensile strain. These crystals transformed to α and ε martensite. The volume fraction of α martensite was sensitive to the crystal orientation, varying from <0.002 to 0.07 for the $[100]_{\gamma}$ and $[\bar{2}\bar{1}3]_{\gamma}$ tensile axis specimens respectively. A detailed discussion of an experimental method to measure the volume fraction of specific K-S variants is presented.

INTRODUCTION

The objective of this study is to investigate the effects of stress and deformation on the formation of martensite in Fe-15^{w}/oNi-15^{w}/oCr single crystals. This paper will discuss specifically how the orientation dependence of the applied stress controls the formation of specific Kurdjumov-Sachs (K-S) variants in the crystal, the experimental method used to identify and measure the volume fraction of each variant, and compare the mechanical property data of these single crystals to polycrystal data of similar composition. The notation for the deformation and isothermal start temperature of the martensite transformation used in this paper is that adopted in Reference 1.

Patel and Cohen (1953)[2] and Richman and Bolling (1971)[3] showed how the action of an applied stress can aid or hinder the formation of α martensite crystals in the austenite matrix. Calculations were made using Patel and Cohen's model[2] in the same way discussed by Goodchild, et al.[4], in an effort to identify which variants of the potential habit plane would be expected if the crystal was deformed between $M_{d\gamma}$ and $M_{s\gamma}$. However, the experimental results clearly showed that many habits that were favored by the above calculations were not present in the crystal and as shown in the present paper all the α martensite appeared to have the same K-S variant of the orientation relationship. In order to study this apparent singularity associated with the direction of an applied stress, an x-ray experiment was designed[5], using a Schulz goniometer[6], that would allow the experimentor to locate and measure the volume fraction of α martensite in the austenite matrix associated with each variant of the K-S orientation relationship. The procedure was also used to measure the volume fraction of ε martensite associated with each $\{111\}_{\gamma}$ plane in the crystal. The results and discussion of these measurements follow.

The mechanical response of these crystals with various tensile axes pulled between $M_d\gamma$ and $M_s\gamma$ is also of interest. Goodchild, et al.[4] observed in plastically deformed 303 and 305 stainless steel that grains with a tensile axis near $\{001\}\gamma$ contained no α nor ε martensite. The absence of α martensite was also observed in single crystals with a $[100]\gamma$ tensile axis. The Patel and Cohen model[2] explains these results very well. Epsilon martensite was observed in $[100]\gamma$ tensile axis crystals, which is in conflict with the polycrystalline studies. An explanation of these polycrystalline results based on the observed stress strain curves of single crystals pulled in tension with various tensile axes is presented.

EXPERIMENTAL PROCEDURES

The Fe-15^{w}/oNi-15^{w}/oCr crystals were 32mm in diameter by 160mm long, and were grown by Advanced Materials Research and Development Laboratory of Pratt and Whitney Aircraft[7]. This alloy is a paramagnetic austenite which has a fairly low stacking fault energy (30-40 ergs/cm^2, estimated from data of Breedis and Kaufman)[1]. The cyrstal was homogenized at 1200°C for 72 hours. Sheets 2.5mm thick were cut from crystal, the face of the sheet being parallel to the $(111)\gamma$ or the $(001)\gamma$ planes.

The single crystal slabs were cut from the large crystal with a Norton abrasive disk No. A90 R0R30. The cutting was performed under a continuous flow of kerosene at 6000 RPM. The slabs were surface ground using 0.002mm steps in the grinding operation. The tensile specimens were electropolished, removing a minimum of 0.15mm of material from each surface. The specimens were electropolished with

15% $HClO_3$(60%), 85% acetic acid at 8 volts, maintaining a temperature of 15°C. The rate of removal was 0.10 to 0.15mm/hour, producing a uniform mirror finish.

The initial orientation of the crystals for machining and a recheck of each tensile specimen before testing was performed using the Laue back reflection method. The final orientation of each crystal was measured by locating the three $\{002\}_\gamma$ poles or the four $\{111\}_\gamma$ poles with a Schulz pole figure goniometer[6] mounted on a Norelco diffractometer. All orientation measurements are estimated to be accurate to ±0.5 degree.

Tensile tests were performed with an Instron Model T-M testing machine. The specimens were gripped, using block type grips with universal action to aid in critical alignment of the system. The testing temperature was maintained by liquid baths. All temperature measurements were made using a copper-constantan thermocouple with 0°C reference junction. The final dimensions of the tensile specimens were measured with an optical micrometer, which has a resolution of better than 0.002mm. However, because the corners of the specimens were rounded due to electropolishing, the accuracy of the measured cross-sectional area is estimated to be 3%. This represents the largest error in the data required for stress measurements. All strain measurements were based on crosshead velocity. Only plastic strains are reported in this paper.

The identification of the α martensite variants of the K-S orientation relationship was accomplished as follows: If single crystals of α martensite form in a single crystal matrix of austenite,

the variants of the orientation relation which form can be located and identified by using pole figure techniques. The angular rotations of the pole figure goniometer allow the experimentor to scan the total volume of the crystal quickly, and the distribution of any pole $\{hkl\}\alpha$ was found simply by setting the diffractometer angle to the appropriate 2θ value, as calculated from Bragg's Law. For this study, the distributions of $\{002\}\alpha$ and $\{10\bar{1}1\}\varepsilon$ poles were measured. They were selected because of their high symmetry and the fact that these poles can be scanned without the problem of overlapping reflections. Iron $K\alpha$ radiation was used for these measurements.

Idealized pole figures were generated showing the distribution of $\{002\}\alpha$ and $\{10\bar{1}1\}\varepsilon$ martensite poles on a $(111)\gamma$ stereographic projection. All K-S variants can be resolved and the four resolvable ε variants can be identified. The resulting idealized distributions of $\{002\}\alpha$ poles for the 24 variants of the K-S orientation relationship and the four orientations of the $\{10\bar{1}1\}\varepsilon$ poles are plotted in Figs. 1 and 2 respectively on a $(111)\gamma$ stereographic projection. The identification of the symbols and numbers on Figs. 1 and 2 are given in Table I. In order to identify a particular variant, the experimental observations are superimposed on to these figures. The correlation between the experimental and calculated positions of a martensite pole was outstanding. After experience with the method developed, the pole figure scan was dropped in favor of the following procedure:

1) The crystal was mounted on the pole figure goniometer and the $\{111\}\gamma$ or $\{001\}\gamma$ poles were located and plotted on a stereographic projection. This established the exact specimen orientation.

2) The idealized pole figures showing the $\{002\}\alpha$ and $\{10\bar{1}1\}\varepsilon$ poles were rotated along great circles to the exact specimen orientation.

3) The goniometer angles for specific α or ε poles were measured from the stereographic projections.

4) The integrated intensity of the α or ε peak was measured if the phase was in fact present. This procedure worked so well that when α or ε martensite was present, the measured goniometer setting was always within 1° of the position of maximum intensity.

The usual procedure used to calculate volume fraction of ε and α martensite is discussed by Cullity.[9] Because of the highly mosaic structure of the deformed crystals, the x-ray intensity measurement was made by holding 2θ for the $\{hkl\}$ reflection of interest constant, and then rocking the crystal through the peak. The speed of rocking the crystal was 0.625 degree per minute. The total integrated intensity was corrected for background and calculations made in the conventional manner[5,9].

One $\{002\}\alpha$ pole for each of the 24 K-S variants is found in the circular distribution around one of the three rectangular clusters of poles seen in Fig. 1. When adjacent variants were present in this region, the peaks for the two $\{002\}\alpha$ poles tend to overlap. In all cases where a second pole for a particular variant was independently observable, the integrated intensity was recorded. A 5% difference in the integrated intensities was typical for the majority of examples where two poles were resolvable. For several pole pairs measured, differences as large as 20% were observed. However, the larger differences in integrated intensities were associated with the low

volume fraction variants. Although no specific claim will be made as to accuracy of these measurements, agreement to within 10% of the total volume fraction of α martensite measured from optical micrographs was achieved. The precision of the volume fraction measurement for any single pole was about 1% and the resolution was of the order of 0.001 (0.1% martensite). The central 1/3 of the surface area of the gauge section was used for all measurements.

EXPERIMENTAL RESULTS

The stress-strain data for $[\bar{1}\bar{1}2]_\gamma$ and $[\bar{2}\bar{1}3]_\gamma$ tensile axis samples at several temperatures are given in Figs. 3 and 4 to illustrate the mechanical behavior of these crystal above and below Md_γ. There appears to be no specific value for Md_γ; Md_γ being a function of the resolved shear stress on the potential α martensite habit planes Specimens tested to 10% tensile strain at 273° and 242°K did not transform to α martensite, but specimens tested in the region of 185°K transformed to an acicular structure consisting of both the ε and α phases (See Fig. 6). The formations of the α phase causes a large reduction in flow stress at this strain rate.

Quantitive volume fraction measurements of ε and α martensite were made on tensile specimens with $[100]_\gamma$, $[\bar{1}\bar{1}2]_\gamma$, $[\bar{2}\bar{1}3]_\gamma$ and $[1\bar{1}0]_\gamma$ tensile axes. These tensile specimens were tested in the region of 185°K to 5% tensile strain. The stress strain curves are given in Fig. 5 and the volume fraction measurements tabulated in Table II. A light metallographic study of the $[\bar{2}\bar{1}3]_\gamma$ tensile axis sample showing the martensite microstructure on the $(\bar{1}11)_\gamma$, $(01\bar{1})_\gamma$, and the $(\bar{2}11)_\gamma$ surfaces are given in Fig. 6. This study uniquely identifies the

acicular shape of the α martensite crystals. The transformation shear of the α martensite formed in this alloy is a slip shear. No twins were observed within the needles except in regions of nearly 100 percent martensite. An electron micrograph showing the dislocated structure of the α martensite is given in Fig. 7.

In all cases ε martensite was observed only on planes that slipped. This was confirmed by comparing slip planes defined by slip traces on two perpendicular surfaces to the x-ray measurements. If slip occurs on a particular $\{111\}_\gamma$ plane, ε martensite was always present as $\{111\}_\gamma \parallel \{0001\}_\varepsilon$. Slip is possible on only two systems for the $[\bar{1}\bar{1}2]_\gamma$ tensile axis sample. Because the crystals were two degrees from the exact $[\bar{1}\bar{1}2]_\gamma$ tensile axis, the $(1\bar{1}1)_\gamma$ $[\bar{1}01]_\gamma$ system was favored producing twice the quantity of ε on the $(1\bar{1}1)_\gamma$ plane than was observed on the $(\bar{1}11)_\gamma$ plane. The majority of the α martensite was also associated with the $(1\bar{1}1)_\gamma$ slip plane and the $[\bar{1}01]_\gamma$ slip direction. An ideal $[\bar{1}10]_\gamma$ tensile axis specimen should slip on two planes; four slip systems. However, a one degree deviation from the $[\bar{1}10]_\gamma$ was sufficient to confine slip to the $(1\bar{1}1)_\gamma$ $[\bar{1}01]_\gamma$ and $(1\bar{1}1)_\gamma$ $[011]_\gamma$ systems. The α martensite was evenly distributed between the K-S variants containing the $[\bar{1}01]_\gamma$ and $[011]_\gamma$ slip directions. The $[100]_\gamma$ sample generated slip on only two systems, the $(1\bar{1}1)_\gamma$ $[110]_\gamma$ and $(111)_\gamma$ $[1\bar{1}0]_\gamma$. Almost no α martensite was observed in this sample and the volume fraction of ε martensite was also less than in other orientations (See Table II). It is clear from the data in Table II that the K-S variants favored in plastically deformed austenite crystals are those associated with both the slip plane and slip direction.

DISCUSSION

Experimental Method

The experimental application of pole figure methods to study the stress dependence on the orientation relationship is believed to be new. The method allows the researcher to measure the presence of a specific K-S variant of a martensite and its volume fraction providing the martensite is dislocated and not twinned.

Some twins exist in the austenite prior to transformation. However, twinning of the austenite will not change the position of the $\{001\}\alpha$ poles for any of the 24 possible K-S variants. By inspection of Fig. 1, one can see that twinning of the austenite on $\{111\}\gamma$ planes causes superposition of $\{001\}\alpha$ martensite poles of the same K-S variant. This in itself will not change the accuracy of the volume fraction measurement nor affect the identification of the specific martensite variants present.

Twinning of the martensite (the inhomogeneous shear) on the other hand causes a much more difficult problem. (Although transformation twinning was not present in this alloy (Fig. 7), a discussion of the problem is presented so that difficulties that will arise when the experimental method is applied to twinned martensite systems is understood.) Consider the $(111)\gamma \parallel (110)\alpha$ set of six K-S variants. This is the set in Fig. 1 identified as $\boxdot_i$. The martensite crystal could shear on either the $[\bar{1}11]\alpha$ or $[1\bar{1}1]\alpha$ direction in this example. If the mode of deformation is twinning, the composition plane will be $(1\bar{1}2)\alpha$ for the $[\bar{1}11]\alpha$ shear direction, or the composition plane will be the $(\bar{1}12)\alpha$ for the $[1\bar{1}1]\alpha$ shear direction.

The results of twinning the crystal, first assuming the shear direction in the martensite is the <111>α direction specified for each K-S variant $\boxdot_1$, $\boxdot_2$,.... $\boxdot_6$ (See Table I), are given in Fig. 8. For example for $\boxdot_1$, the $[\bar{1}01]_\gamma \parallel [\bar{1}11]_\alpha$, the composition plane is $(1\bar{1}2)_\alpha$. Then for the case $[\bar{1}01]_\gamma \parallel [1\bar{1}1]_\alpha$ the composition plane is $(\bar{1}12)_\alpha$. If Fig. 8 is superimposed upon Fig. 1, superposition of cube poles for the twinned and untwinned cases which are not in fact the same K-S variant are observed. Note for the six K-S variants associated with the $(111)_\gamma \parallel (110)_\alpha$ planes, that twin superposition occurs in pairs. In other words if $\boxdot_1$ is twinned forming $\boxdot_{T1}$, the position of $\boxdot_{T1}$ poles superimpose onto $\boxdot_2$ poles. Likewise if $\boxdot_2$ poles are twinned, the $\boxdot_{T2}$ poles superimpose upon $\boxdot_1$ poles. This pair matching occurs for every possible set.

Therefore, if $\boxdot_1$ is present and is twinned one would observe, experimentally, intensity at both the $\boxdot_1$ and $\boxdot_2$ positions. One would not know by x-ray methods alone if only one variant is present and is twinned, or both present and twinned. This does imply, however, that if only one pole of the pair was observed, it must not be twinned and it is therefore uniquely identified. Also it is observed that quantitative volume fraction measurements of specific K-S variants cannot be made using the cube poles if the martensite crystals are twinned with the <111>α shear direction being the K-S correspondence vector. Thin foil electron microscopy can of course resolve this difficulty and will be described in a later paper.[8]

As was pointed out, there are two possible twinning planes in any {110}α orientation. For the (110)α case being discussed, the martensite variant $[\bar{1}01]_\gamma \parallel [\bar{1}11]_\alpha$ could also be sheared in the $[1\bar{1}1]_\alpha$ direction with a $(\bar{1}12)_\alpha$ composition plane. If this second twin is considered, a

new set of cube poles are generated (shown in Fig. 9) which do not superimpose upon the untwinned α martensite crystals (Fig. 1). However, $\{001\}_\gamma$ poles in these twin positions were not observed experimentally in a Fe-35.5^w/o Ni alloy that was heavily twinned using the x-ray pole figure method.[5] This indicates that all twinning in the Fe-35.5^w/oNi alloy must be associated with the $\langle 111\rangle_\alpha$ shearing direction that is in correspondence with the K-S variant.

The accuracy of the volume fraction measurements was in general disappointing. The 5% difference in integrated intensity observed between two different $\langle 001\rangle_\alpha$ martensite poles of the same crystal orientation was much larger than expected. The most likely source of error is due to the fact that slip is not homogeneous and consequently the intensity distribution is non-symmetrical. This would cause different values of the integrated intensity for different directions of scan over the peak. The fact that the total volume fraction obtained using the x-ray method agrees fairly well with the light optical metallographic results indicates that the method is valid.

The mechanical property data of these single crystals (Fig. 3,4, and 5) help to explain the orientation dependence of ε and α martensite formation in the polycrystal data presented by Goodchild, et al.[4] for textured 301 and 305 austenitic stainless steel. They observed that the formation of ε and α martensite was inhibited in grains with the $\langle 001\rangle_\gamma$ parallel to the tensile axis. Grains with the $\langle 110\rangle_\gamma$ parallel to the tensile axis contained ε and moderate amounts of α martensite. Grains with one of the $\langle 123\rangle_\gamma$ parallel to the tensile axis contained ε martensite and the maximum amounts of α martensite. The single crystal

results given in Table II follow these same trends for α martensite, but not for ε martensite. A reduction of ε martensite was observed in the $[100]_\gamma$ tensile axis specimen, but not to the extent suggested by the polycrystalline studies[4]. The reason almost no ε martensite is present in grains with the $\langle 100 \rangle_\gamma$ parallel to the tensile axis in polycrystal samples may be due to the orientation dependence of the flow stress observed in single crystals tested between Md_γ and Ms_γ, (Figs. 3 and 4). For single crystals, the yield and flow stress is reduced significantly when the $\gamma \rightarrow \alpha$ transformation can proceed with ease. A single crystal with a $[100]_\gamma$ tensile axis is not producing α martensite, consequently a higher yield and flow stress are observed (Fig. 5). Epsilon martensite is not found in grains with the $\langle 001 \rangle_\alpha$ parallel to the tensile axis in polycrystalline austenitic stainless steel because under these deformation conditions the stress in these grains does not exceed the CRSS for slip.

The reason α is not forming appears to be related to the work done by the stress which can either aid or hinder the $\gamma \rightarrow \alpha$ transformation. The orientation dependence of α martensite formation follows from the criterion established by Patel and Cohen[2] showing how the work done by an external stress resolved on the habit plane (τ) and the normal to the habit plane (σ_n) of the martensite plate can raise the martensite start temperature. The work done by the stress is written as

$$U = \tau\gamma_0 + \sigma_n\varepsilon_0$$

where γ_0 is the transformation shear in the habit plane and ε_0 is the transformation shear normal to the habit plane. The values of γ_0 and

ε_0 used were 0.20 and 0.04 respectively. Very simply, the effect on Ms_γ due to an applied stress is

$$\Delta F^{\gamma\to\alpha} @ Ms_\gamma = \Delta F^{\gamma\to\alpha} @ Md_\gamma + U$$

where $Ms_\gamma < Md_\gamma$. The magnitude of U depends upon the magnitude of the resolved shear stress τ and the normal stress σ_n on the potential martensite habit plane.

Goodchild et al.[4] show that the magnitude of U/σ where σ is the applied stress will indicate which martensite crystals should be favored due to the applied stress. The larger U/σ, the more the stress aids the formation of a particular martensite crystal. If it is assumed that the habit plane is the $\{112\}_\gamma$ and shear direction is the $\langle 110\rangle_\gamma$[4,10], crystals with the largest value of U/σ are not always observed experimentally in this alloy.

Based upon U/σ calculations, the crystal with $[\bar{2}\bar{1}3]_\gamma$ tensile axis should favor about equally ($U/\sigma \approx 0.13$) martensite crystal formation for the following habit plane-shear directions: $(\bar{1}\bar{1}2)_\gamma$ $[\bar{1}10]_\gamma$, $(\bar{2}11)_\gamma$ $[0\bar{1}1]_\gamma$, $(\bar{1}12)_\gamma$ $[\bar{1}\bar{1}0]_\gamma$, and $(\bar{2}\bar{2}1)_\gamma$ $[011]_\gamma$. Only the $(\bar{2}11)_\gamma$ $[0\bar{1}1]_\gamma$ of this set was observed experimentally. This result is clearly seen in Fig. 6A, which was sectioned to show the $(\bar{2}11)_\gamma$ surface. Because the austenite shear direction in the $[\bar{2}\bar{1}3]_\gamma$ tensile axis crystal is the $[0\bar{1}1]_\gamma$, it was expected to find the long axis of needles near the $[0\bar{1}1]_\gamma$ in the $(\bar{2}11)_\gamma$ plane. This clearly was the result. Fig. 6B shows the same crystal sectioned to expose the $(01\bar{1})_\gamma$ plane. It is clear that α Martensite needles cut the surface in packets that appear to be confined to the $(\bar{1}11)_\gamma$ plane. Electron microscopy of $(01\bar{1})_\gamma$ foils showed that the α martensite is confined on two sides by large ε martensite sheets that are parallel

to the $(\bar{1}11)_\gamma$ plane[8]. Fig. 6C is the same crystal cut to expose the $(\bar{1}11)_\gamma$ plane. The α martensite typically appears as small, highly transformed regions, that are widely separated in the austenite matrix. Accurate habit plane measurements[8] from optical micrographs show that the systems $(\bar{2}11)_\gamma\ [0\bar{1}1]_\gamma$, $(12\bar{1})_\gamma\ [101]_\gamma$, $(1\bar{1}2)_\gamma\ [\bar{1}\bar{1}0]_\gamma$, and $(211)_\gamma\ [0\bar{1}\bar{1}]_\gamma$ with $U/\sigma = 0.13$, 0.08, 0.08 and 0.04 respectively are formed when the crystal is deformed plastically with the $[\bar{2}\bar{1}3]_\gamma$ tensile axis.

The difficulty at the present time is that the present model[2] favors the presence of α martensite habit planes that are not experimentally observed in this alloy. The metallographic results show that the austenite matrix is partitioned by the ε phase as sheets parallel to the $\{111\}_\gamma$ slip planes. This partitioning appears to control both the size of the acicular α martensite crystals and the plane on which the α martensite crystals can form. Such partitioning is not accounted for in the model. If all the α martensite crystals were to form with the habit planes suggested by the theory, many needles would have to cut through the ε martensite sheet. This event has not been observed. Therefore, it is not surprising, because of ε martensite partitioning, that all the α martensite that forms due to the deformation has the $(110)_\alpha$ plane always parallel to the $\{111\}_\gamma$ slip plane(s), and that the direction of shear in the austenite is playing a dominant role in determining the specific K-S variant that is present.

CONCLUSIONS

1. The variant of the K-S orientation relation for α martensite present in Fe-15^{w}/oNi-15^{w}/oCr single crystals was always the variant that contained both the austenite slip plane and slip

direction. This characteristic was true for both single and multiple slip orientations.

2. The experimental method described can be used to identify each K-S variant of α martensite in the single crystals and measure its volume fraction providing the martensite is not twinned. Even if the martensite is twinned, useful information about the behavior of the γ-α transformation can be obtained.

3. The reason that grains with a cube axis near the tensile axis of polycrystalline austenite stainless steels do not contain ε or α martensite can be explained based upon single crystal results. It is clear that when the γ-α transformation can proceed, the stress required for slip is reduced. If the $\langle 001 \rangle_\gamma$ is near the tensile axis, the $\gamma \rightarrow \alpha$ transformation cannot proceed. The bulk of plastic deformation in the polycrystal proceeds in grains where the $\gamma \rightarrow \alpha$ transformation occurs, leaving the $\langle 001 \rangle_\gamma$ grains parallel to the tensile axis undeformed. This explains that no ε or α martensite was observed experimentally in these grains by Goodchild, et al.[4]

4. Many α martensite crystal orientations that should be favored as predicted by the Patel-Cohen model are not observed experimentally. This is explained by the following; because the γ-ε transformation occurs before the γ-α transformation due to plastic deformation, the austenite matrix becomes partitioned by ε plates parallel to the slip plane(s). This partitioning blocks the formation of needles with energetically favored habit planes. The majority of needles that are forming, even under the restriction of partitioning, have high U/σ

values and thus tends to support the basic concept of the model.

ACKNOWLEDGMENTS

The authors wish to thank Professor R. Wenk for the use of his x-ray equipment and discussions related to the volume fraction measurements. Also many thanks are due to Lutgard de Jonghe and Omer van der Biest for helpful discussions. The alloy single crystals used in this study were grown by the Advanced Materials Research and Development Laboratory of Pratt and Whitney Aircraft. This work was performed under the auspices of the United States Atomic Energy Commission.

REFERENCES

1. J. F. Breedis and L. Kaufman, "Formation of HCP and BCC Phases In Austenitic Iron Alloys", Met. Trans., 1971, Vol. 2, pp. 2359-2371.
2. J. R. Patel and M. Cohen, "Criterion for the Action of Applied Stress In the Martensite Transformation", Acta Met., 1953, Vol. 1, pp. 531-538.
3. R. H. Richman and G. F. Bolling "Stress Deformation and Martensitic Transformation", Met. Trans., 1971, Vol. 2, pp. 2451-2462.
4. D. Goodchild, W. T. Roberts, and D. V. Wilson, "Plastic Deformation and Phase Transformation in Textured Austenitic Stainless Steel", Acta Met., 1970, Vol. 18, p. 1137.
5. G. A. Stone, "On The Deformation Induced Martensite Transformation In Fe-Ni- and Fe-Ni-Cr Single Crystals", M.S. Thesis, Lawrence Berkeley Laboratory Report LBL-134, University of California, Berkeley, 1971.
6. L. G. Schulz, "A Direct Method To Determining Preferred Orientation of Flat Reflection Sample Using A Geiger Counter X-ray Spectrometer", J.A.P., 1949, Vol. 20, pp. 1030-1033.
7. Courtesy of B. H. Kear, Pratt and Whitney, Connecticut.
8. G. A. Stone and G. Thomas, "The Microstructure of Fe-Ni-Cr Martensite", University of California, Berkeley, unpublished research, 1973.
9. B. C. Cullity, Elements of X-ray Diffraction, p. 388, Addison-Wesley, Pergamon Press, Oxford, 1965.
10. P. M. Kelly, "The Martensite Transformation in Steels With Low Stacking Fault Energy", Acta Met., 1965, Vol. 13, p. 635.

TABLE I

The 24 variants of the Kurdjumov-Sachs orientation relationship and the 4 γ-ε interfaces. Symbols γ, α, ε refer to f.c.c., b.c.c. and h.c.p. crystals respectively.

BCC Fig. 1

Symbol	Variant	
[·]	1. $(111)_\gamma \parallel (110)_\alpha$;	$[\bar{1}01]_\gamma \parallel [\bar{1}11]_\alpha$
	2.	$[\bar{1}01]_\gamma \parallel [\bar{1}1\bar{1}]_\alpha$
	3.	$[\bar{1}10]_\gamma \parallel [\bar{1}11]_\alpha$
	4.	$[\bar{1}10]_\gamma \parallel [\bar{1}1\bar{1}]_\alpha$
	5.	$[01\bar{1}]_\gamma \parallel [\bar{1}11]_\alpha$
	6.	$[01\bar{1}]_\gamma \parallel [\bar{1}1\bar{1}]_\alpha$
[X]	1. $(\bar{1}11)_\gamma \parallel (110)_\alpha$;	$[\bar{1}\bar{1}0]_\gamma \parallel [\bar{1}11]_\alpha$
	2.	$[\bar{1}\bar{1}0]_\gamma \parallel [\bar{1}1\bar{1}]_\alpha$
	3.	$[\bar{1}0\bar{1}]_\gamma \parallel [\bar{1}11]_\alpha$
	4.	$[\bar{1}0\bar{1}]_\gamma \parallel [\bar{1}1\bar{1}]_\alpha$
	5.	$[01\bar{1}]_\gamma \parallel [\bar{1}11]_\alpha$
	6.	$[01\bar{1}]_\gamma \parallel [\bar{1}1\bar{1}]_\alpha$
[■]	1. $(1\bar{1}1)_\gamma \parallel (110)_\alpha$;	$[\bar{1}01]_\gamma \parallel [\bar{1}11]_\alpha$
	2.	$[\bar{1}01]_\gamma \parallel [\bar{1}1\bar{1}]_\alpha$
	3.	$[011]_\gamma \parallel [\bar{1}11]_\alpha$
	4.	$[011]_\gamma \parallel [\bar{1}1\bar{1}]_\alpha$
	5.	$[110]_\gamma \parallel [\bar{1}11]_\alpha$
	6.	$[110]_\gamma \parallel [\bar{1}1\bar{1}]_\alpha$
[+]	1. $(11\bar{1})_\gamma \parallel (110)_\alpha$;	$[011]_\gamma \parallel [\bar{1}11]_\alpha$
	2.	$[011]_\gamma \parallel [\bar{1}1\bar{1}]_\alpha$
	3.	$[\bar{1}10]_\gamma \parallel [\bar{1}11]_\alpha$
	4.	$[\bar{1}10]_\gamma \parallel [\bar{1}1\bar{1}]_\alpha$
	5.	$[101]_\gamma \parallel [\bar{1}11]_\alpha$
	6.	$[101]_\gamma \parallel [\bar{1}1\bar{1}]_\alpha$

HCP Fig. 2

(·)	1. $(111)_\gamma \parallel (0001)_\varepsilon$
	2. $(1\bar{1}1)_\gamma \parallel (0001)_\varepsilon$
	3. $(\bar{1}11)_\gamma \parallel (0001)_\varepsilon$
	4. $(11\bar{1})_\gamma \parallel (0001)_\varepsilon$

TABLE II

Summary of volume fraction measurements for Fe-15^{w}/o Ni-15^{w}/o Cr alloy tested to 5% tensile strain at 185°K

Symbol+		Variant		$[\bar{2}\bar{1}3]$ Tensile axis C_α	$[\bar{1}\bar{1}2]$ Tensile axis C_α	$[\bar{1}10]$ Tensile axis C_α	$[100]$ Tensile axis C_α
X	1	$(\bar{1}11)_\gamma \parallel (110)_\alpha$;	$[\bar{1}\bar{1}0]_\gamma \parallel [\bar{1}11]_\alpha$	0.0072	0.0018	not observed	
X	2		$[\bar{1}\bar{1}0]_\gamma \parallel [\bar{1}1\bar{1}]_\alpha$	0.0033	0.0006	not observed	Same
X	3		$[\bar{1}0\bar{1}]_\gamma \parallel [\bar{1}11]_\alpha$	0.0011	not observed	not observed	very weak
X	4		$[\bar{1}0\bar{1}]_\gamma \parallel [\bar{1}1\bar{1}]_\alpha$	not observed	not observed	not observed	peaks observed
X	5		$[01\bar{1}]_\gamma \parallel [\bar{1}11]_\alpha$	0.0137*	≈0.0006	not observed	just above back-
X	6		$[01\bar{1}]_\gamma \parallel [\bar{1}1\bar{1}]_\alpha$	0.0421*	0.0019	not observed	ground
■	1	$(1\bar{1}1)_\gamma \parallel (110)_\alpha$;	$[\bar{1}01]_\gamma \parallel [\bar{1}11]_\alpha$	not observed	0.0132*	0.0044	
■	2		$[\bar{1}01]_\gamma \parallel [\bar{1}1\bar{1}]_\alpha$	not observed	0.0056	0.0105*	
■	3		$[011]_\gamma \parallel [\bar{1}11]_\alpha$	not observed	not observed	0.0112*	
■	4		$[011]_\gamma \parallel [\bar{1}1\bar{1}]_\alpha$	not observed	not observed	0.0032	
■	5		$[110]_\gamma \parallel [\bar{1}11]_\alpha$	not observed	0.0020	≈0.0003	
■	6		$[110]_\gamma \parallel [\bar{1}1\bar{1}]_\alpha$	not observed	0.0041	not observed	
			TOTAL α	0.674	0.0298	0.0296	≈0.002
				C_ε	C_ε	C_ε	C_ε
⊙	1	$(111)_\gamma \parallel (0001)_\varepsilon$		not observed	not observed	not observed	0.0102
⊙	2	$(1\bar{1}1)_\gamma \parallel (0001)_\varepsilon$		not observed	0.0194	0.0270	0.0045
⊙	3	$(\bar{1}11)_\gamma \parallel (0001)_\varepsilon$		0.0214	0.0091	not observed	not observed
⊙	4	$(11\bar{1})_\gamma \parallel (0001)_\varepsilon$		not observed	not observed	not observed	not observed
			TOTAL ε	0.0214	0.0285	0.0270	0.0147
			TOTAL α + ε	0.0888	0.0583	0.0566	0.0167

* The majority of α martensite is always associated with the active austenite slip plane and direction.

\+ See Figs. 1 and 2

FIGURE CAPTIONS

Fig. 1. Stereographic plot showing the position of the $\{002\}\alpha$ poles for each of the 24 K-S variants in the $(111)_\gamma$ single crystal matrix. See Table I for code of symbols.

Fig. 2. Stereographic plot showing the position of the $\{10\bar{1}1\}\varepsilon$ poles for the γ-ε variants of the orientation relationship in $(111)\gamma$ single crystal matrix. See Table I for code of symbols.

Fig. 3. Fe-15^W/oNi-15^W/oCr $[\bar{1}\bar{1}2]\gamma$ tensile axis stress strain data above and below $Md\gamma$. Arrow indicates specimen was unloaded.

Fig. 4. Fe-15^W/oNi-15^W/oCr $[\bar{2}\bar{1}3]\gamma$ tensile axis stress strain data above and below $Md\gamma$. Arrow indicates specimen was unloaded.

Fig. 5. Fe-15^W/oNi-15^W/oCr $[100]\gamma$, $[1\bar{1}0]\gamma$, $[\bar{1}\bar{1}2]\gamma$, and $[\bar{2}\bar{1}3]\gamma$ tensile axis stress strain data at 185°K showing the orientation dependence of the flow stress. Arrow indicates specimen was unloaded.

Fig. 6. The $[\bar{2}\bar{1}3]\gamma$ tensile axis specimen was sectioned to show (A) the $(\bar{2}11)\gamma$ surface, (B) the $(01\bar{1})\gamma$ surface, and (C) the $(\bar{1}11)\gamma$ surface of the single crystal.

Fig. 7. Electron micrograph showing the dislocated martensite structure.

Fig. 8. Stereographic plot of $\{002\}\alpha$ twin poles for the first six K-S variants given in Table I assuming the twinning shear is K-S correspondence vector. Superposition of this figure into Fig. 1 shows the twin relationship.

Fig. 9. Stereographic plot of $\{002\}\alpha$ twin poles for the first six K-S variants given in Table I assuming the twinning shear is not the K-S correspondence vector. No superposition of twin poles for this twinning shear and the matrix occurs.

0 0 0 0 3 9 0 0 9 2 5

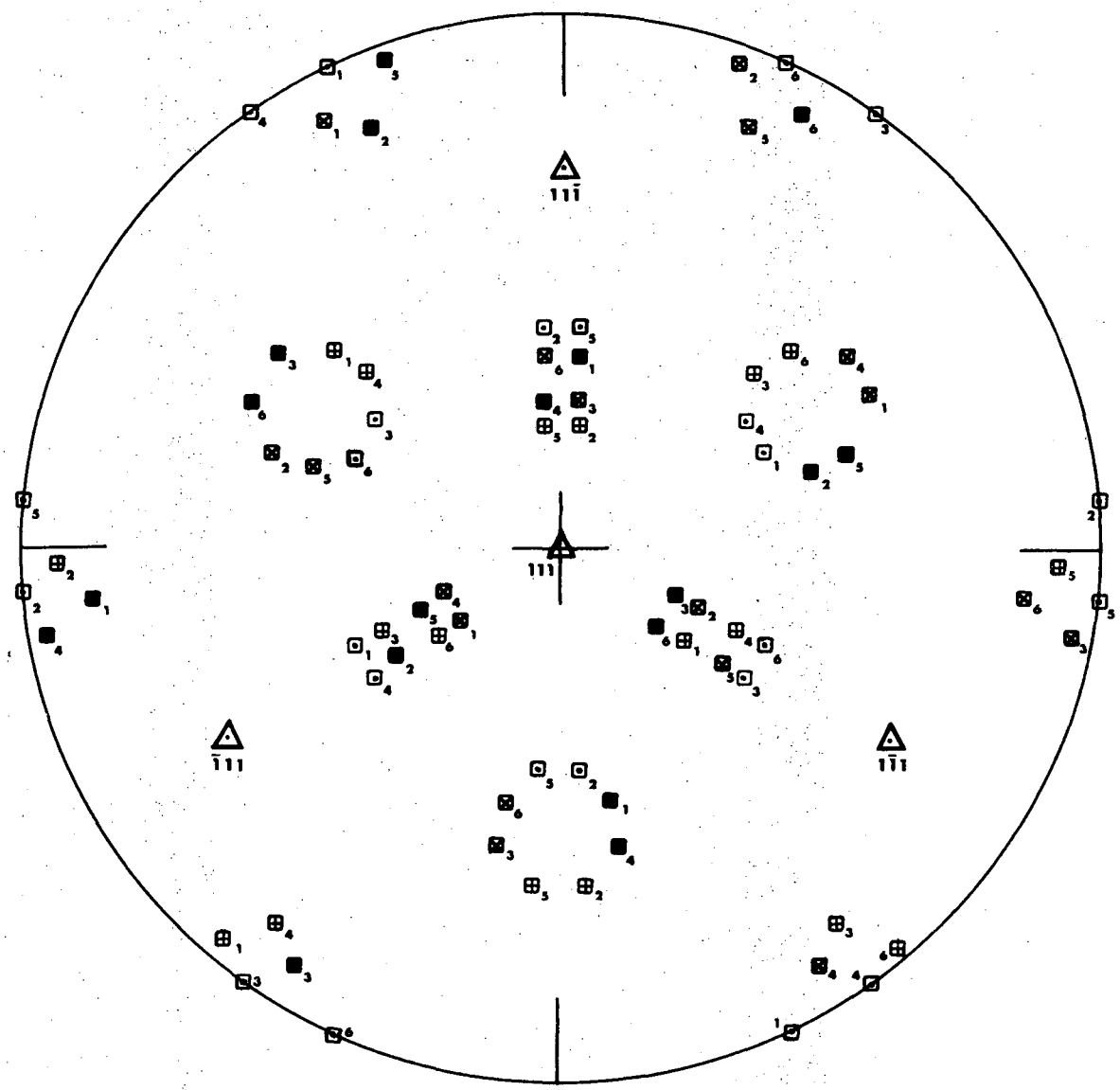

XBL 7011-7050

Fig. 1

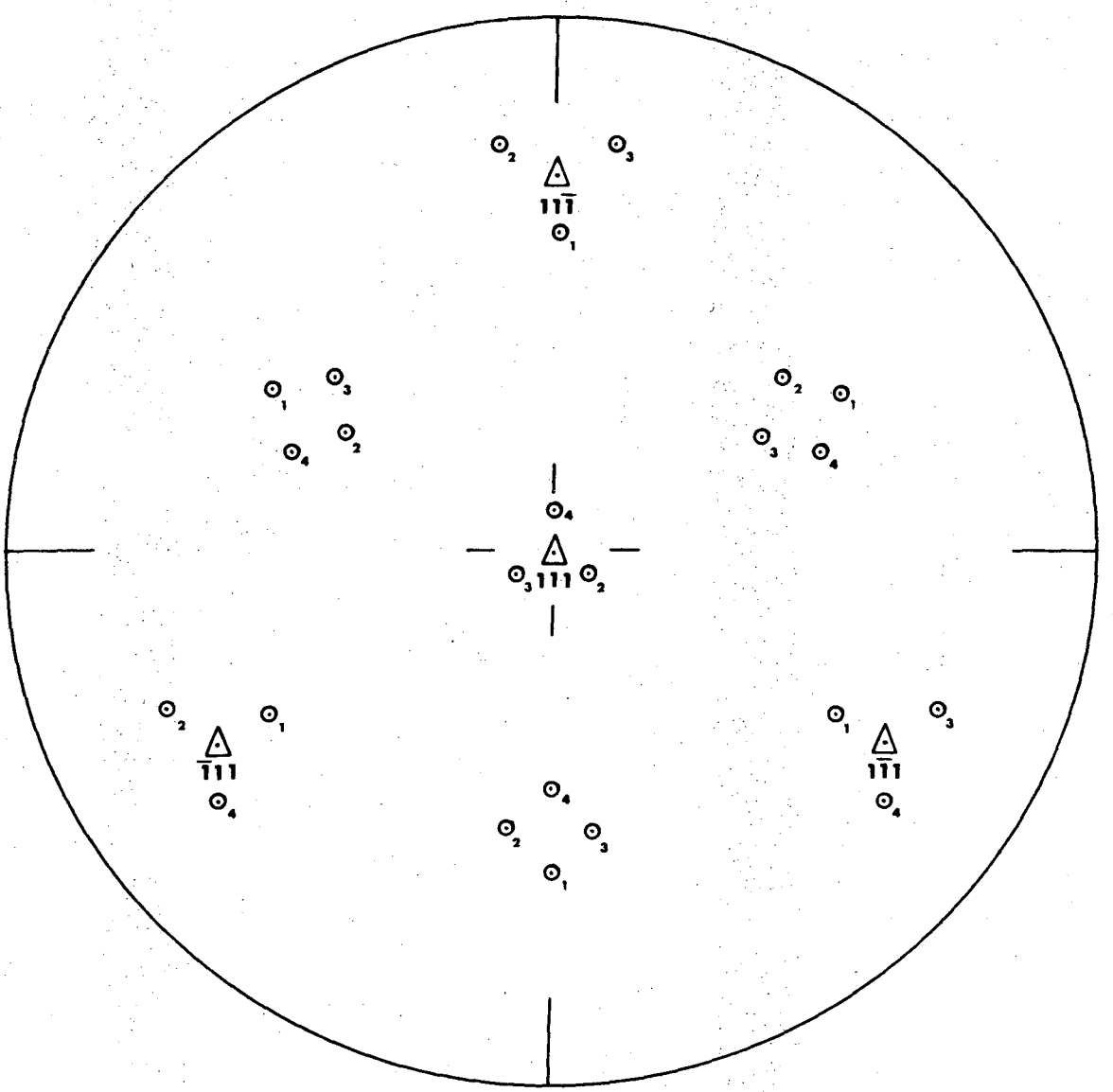

XBL 717-7072

Fig. 2

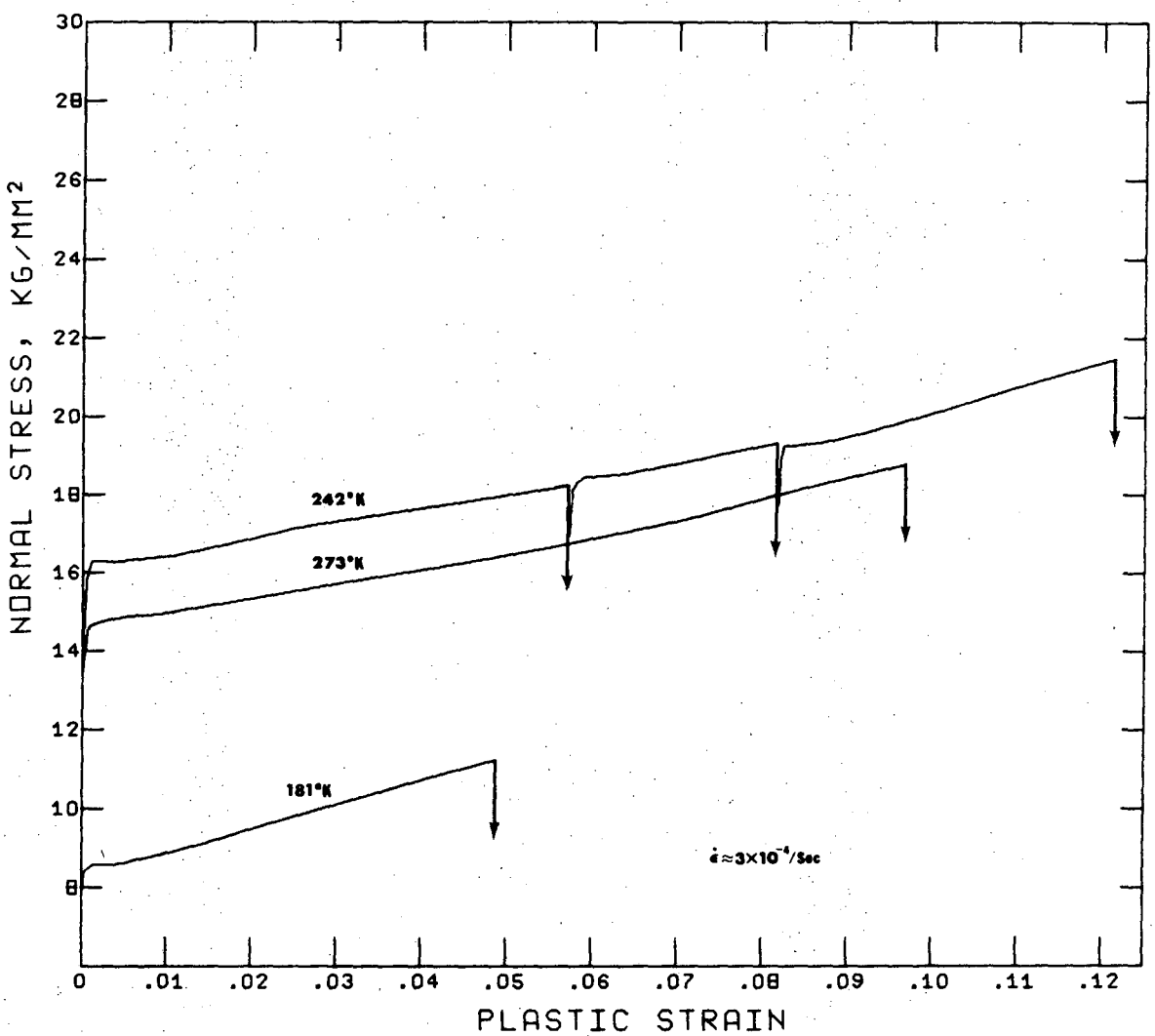

XBL 7011-6953

Fig. 3

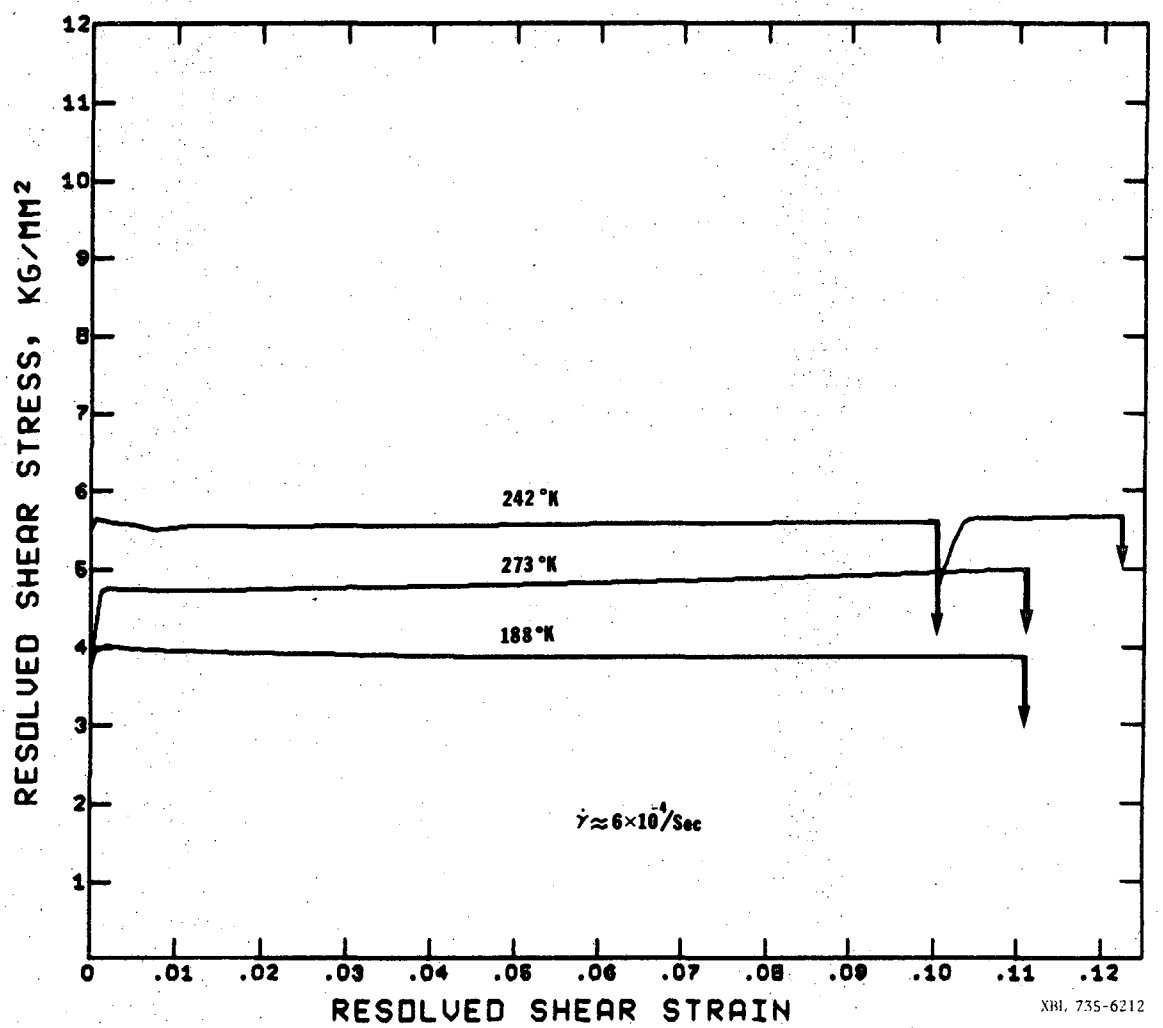
RESOLVED SHEAR STRESS, KG/MM²
RESOLVED SHEAR STRAIN
242 °K
273 °K
188 °K
γ̇≈6×10⁻⁴/Sec
0
.01
.02
.03
.04
.05
.06
.07
.08
.09
.10
.11
.12
1
2
3
4
5
6
7
8
9
10
11
12
XBL 735-6212

Fig. 4

0 0 0 0 3 9 0 5 9 2 6

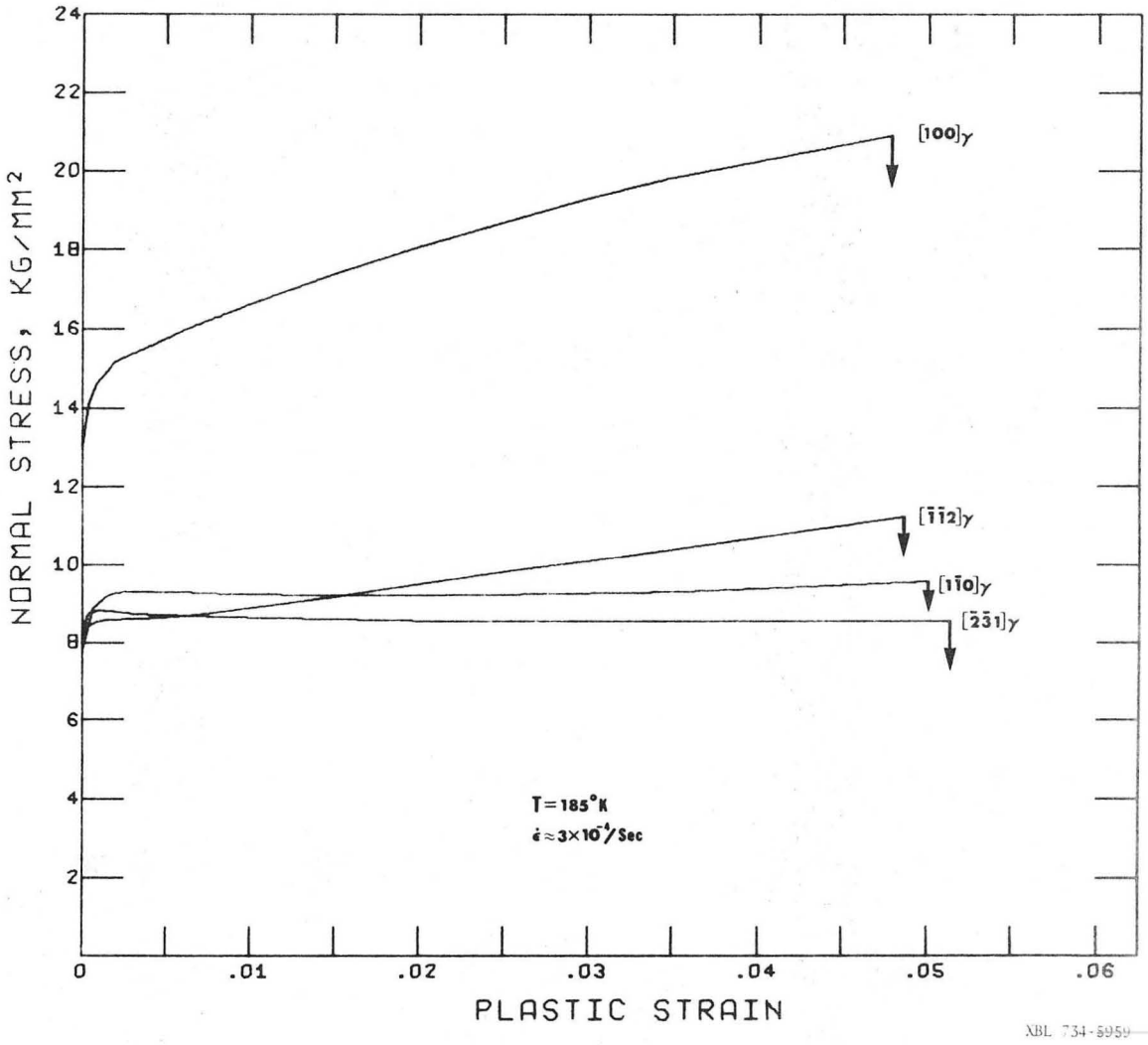

Fig. 5

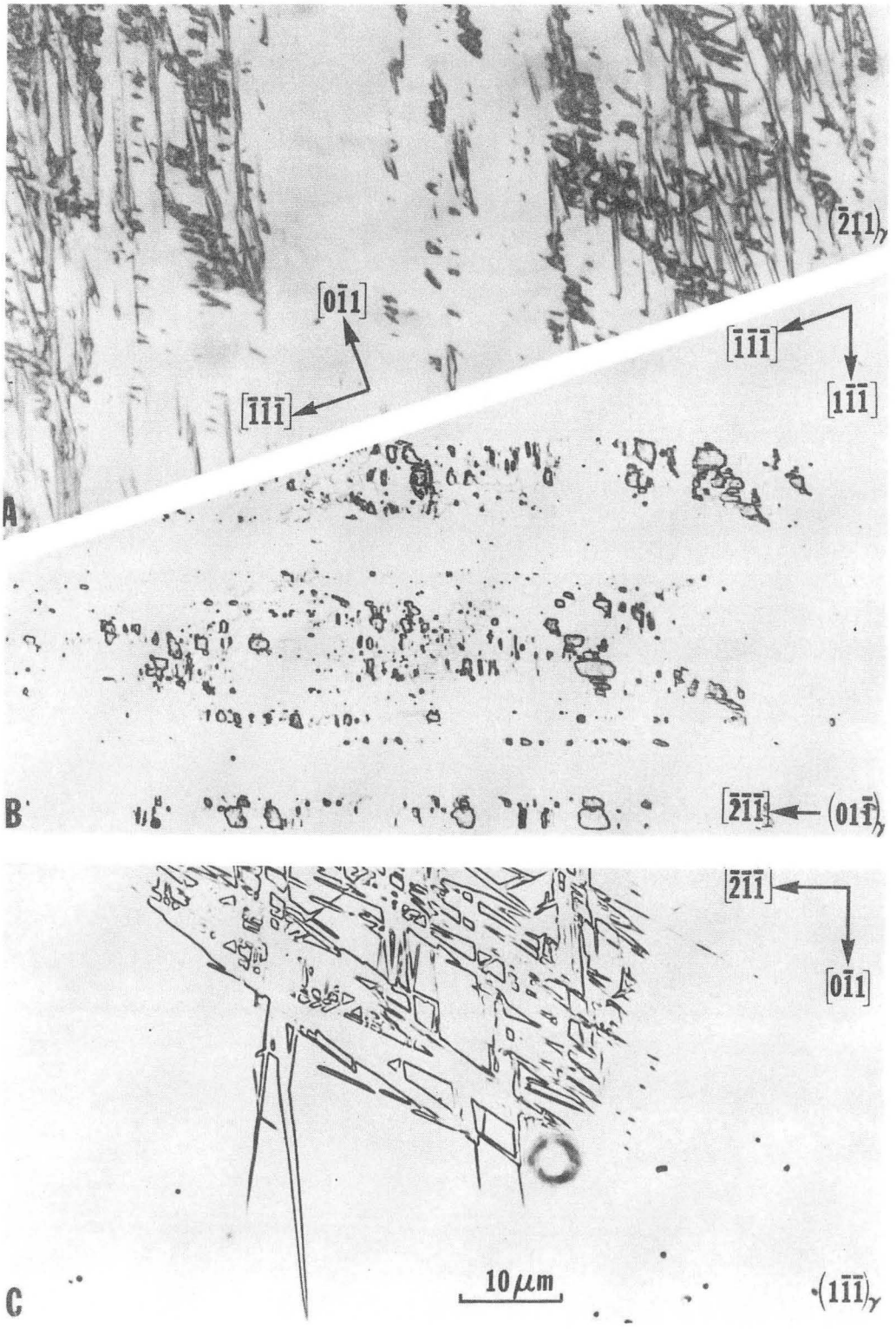

XBB 734-2476

Fig. 6

0 0 0 0 3 9 0 5 9 2 7

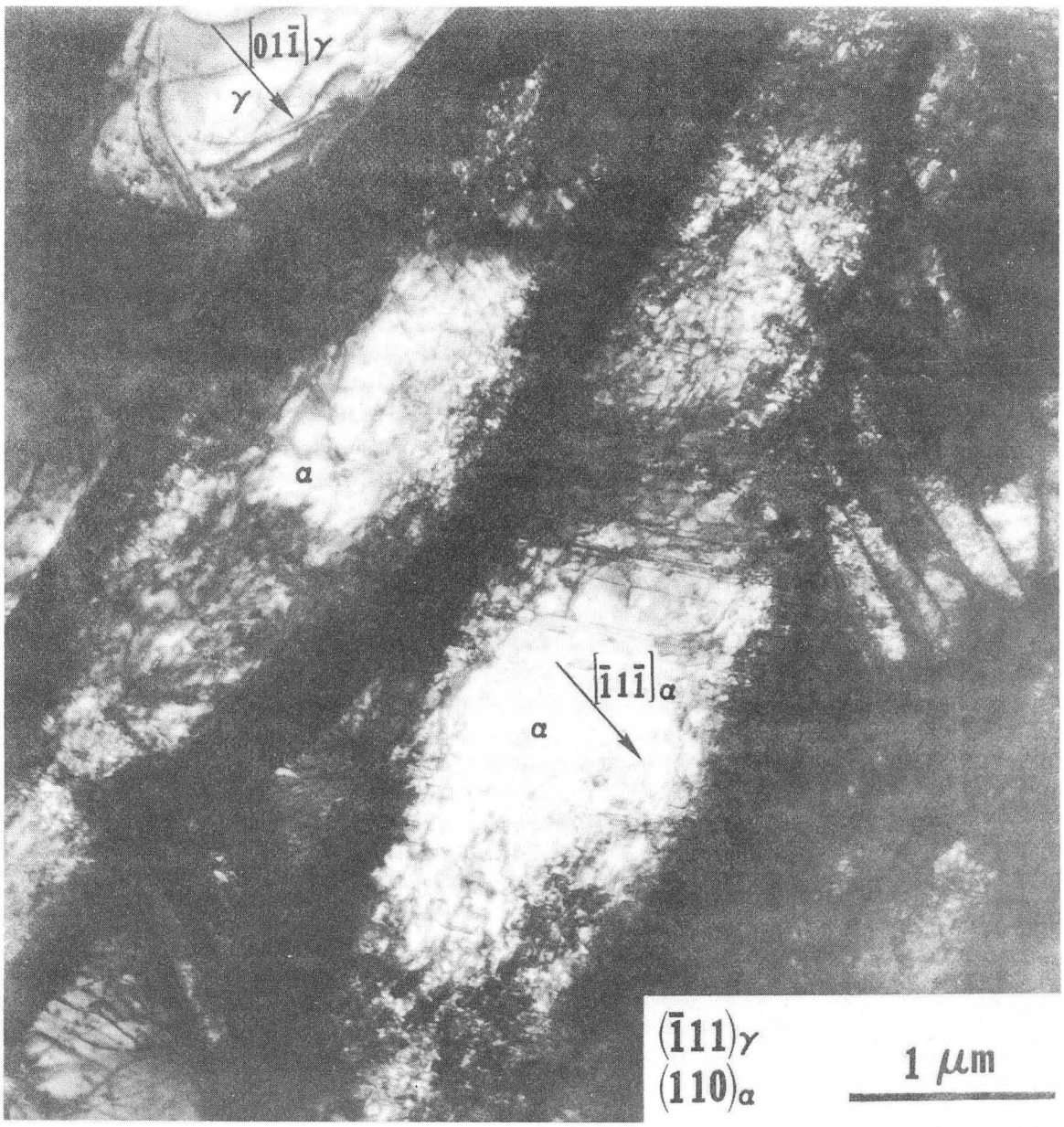

XBB 736-3621

Fig. 7

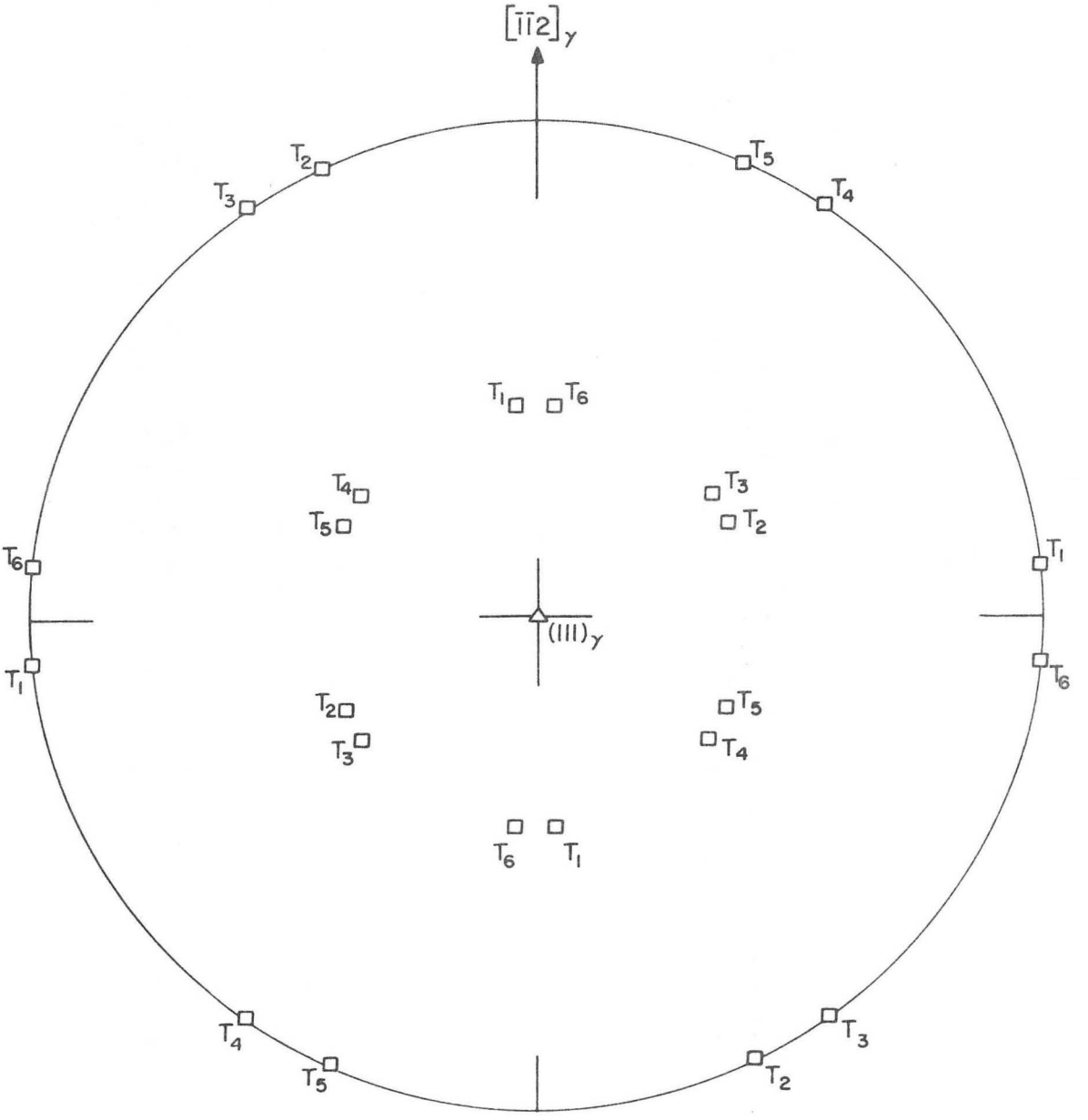

XBL 736-6311

Fig. 8

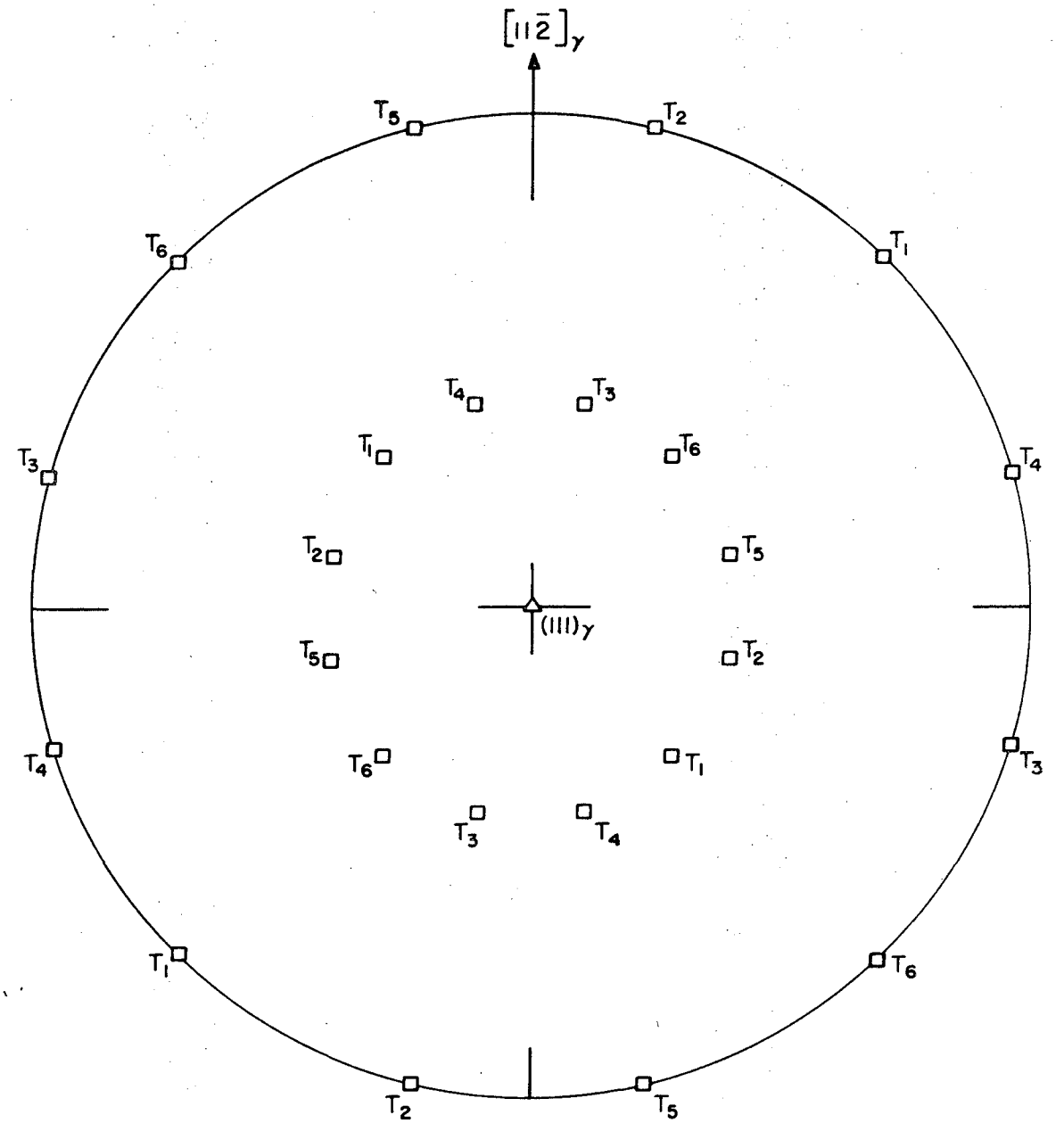

XBL 736-6312

Fig. 9

0 0 0 0 3 9 0 0 7 2 8

UNIVERSITY OF CALIFORNIA

Lawrence Berkeley Laboratory
Berkeley, California

Date: May 15, 1974

ERRATA

TO: All recipients of LBL-1853

FROM: Inorganic Materials Research Division and Technical Information Div.

SUBJECT: LBL-1853, "Deformation Induced Alpha and Epsilon Martensities in Fe-Ni-Cr Single Crystals," Glen Stone and Gareth Thomas, July 1973.

Please make the following corrections on subject report.

Page 28, Figure 8 is corrected -- new copy attached

Page 29, Figure 9 should be deleted along with the caption on page 20.

APPENDIX A -- should be added (copy attached).

0 0 0 0 3 9 0 0 9 2 9

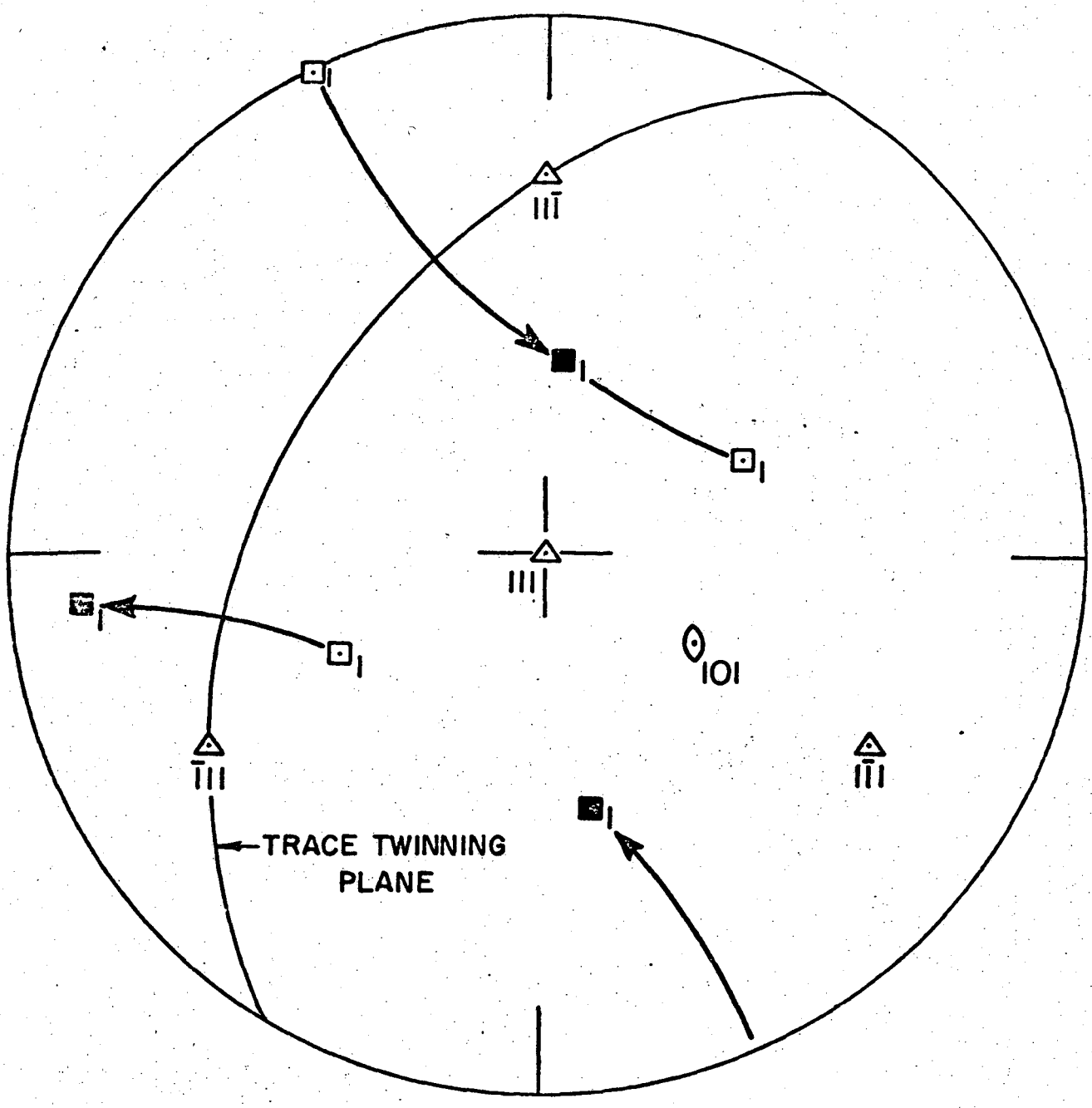

XBL 745-6250

Fig. 8.

Appendix A

Influence of Internal Twinning of α-Martensite

Difficulties can arise when working with alloys in which the martensite is twinned because superposition of different K-S variants will occur.

To illustrate this problem, consider twinning of a martensite crystal having the K.S. variant $(111)_\gamma || (110)_\alpha$; $[\bar{1}01]_\gamma || [\bar{1}11]_\alpha$ which is identified as $\square_1$ in Figure 1 and Table I.

The Bain correspondence for this variant is

$$ {}_\alpha\underline{C}_\gamma = \begin{pmatrix} 0 & 0 & 1 \\ 1 & 1 & 0 \\ 1 & \bar{1} & 0 \end{pmatrix} $$

Twinning will occur on the $(211)_\alpha$ composition plane with the direction of shear being $[\bar{1}11]_\alpha$. The corresponding plane in the austenite is the $(101)_\gamma$. When this variant is twinned, superposition of variant $\square_1$ upon $\blacksquare_1$ occurs. A sterogram is presented in Fig. 8 that demonstrates this property. This superposition of a twinned variant upon an untwinned one occurs for all 24 K-S variants of the orientation relationship.

The experimental method used in this study is complicated if twinning of the martensite occurs. For example if variant $\square_1$ is present and is twinned, one would observe experimentally x-ray diffraction at both $\square_1$ and $\blacksquare_1$ positions. It is not possible by x-ray methods alone to tell if only one variant is present and is twinned, or if both are present either twinned or untwinned. This does imply, however, that if only one pole of the pair was observed, it must not be twinned and it is therefore uniquely identified. Also it is observed that quantitative

volume fraction measurement of specific K-S variants cannot be made using the cube poles if the martensite crystals are twinned. Thin foil electron microscopy can of course resolve this difficulty and will be described in a later paper.[8]

LEGAL NOTICE

This report was prepared as an account of work sponsored by the United States Government. Neither the United States nor the United States Atomic Energy Commission, nor any of their employees, nor any of their contractors, subcontractors, or their employees, makes any warranty, express or implied, or assumes any legal liability or responsibility for the accuracy, completeness or usefulness of any information, apparatus, product or process disclosed, or represents that its use would not infringe privately owned rights.

TECHNICAL INFORMATION DIVISION
LAWRENCE BERKELEY LABORATORY
UNIVERSITY OF CALIFORNIA
BERKELEY, CALIFORNIA 94720